Hydrol. Earth Syst. Sci. Discuss., https://doi.org/10.5194/hess-2019-72
Manuscript under review for journal Hydrol. Earth Syst. Sci.
Discussion started: 13 February 2019

Toward high-spatial resolution hydrological modeling for China: Calibrating the VIC model

Bowen Zhu[1,2], Xianhong Xie[1,2*], Chuiyu Lu[3], Shanshan Meng[1,2], Yi Yao[1,2], Yibing Wang[1,2]

1. State Key Laboratory of Remote Sensing Science, Jointly Sponsored by Beijing Normal University and Institute of Remote Sensing and Digital Earth of Chinese Academy of Sciences, Beijing 100875, China
2. Beijing Engineering Research Center for Global Land Remote Sensing Products, Institute of Remote Sensing Science and Engineering, Faculty of Geographical Science, Beijing Normal University, Beijing 100875, China
3. China Institute of Water Resources and Hydropower Research, State Key Laboratory of Simulation and Regulation of Water Cycle in River Basin, Beijing 100038, China

*Corresponding author: Xianhong Xie (Beijing Normal University, xianhong@bnu.edu.cn)

Abstract

High-resolution hydrological modeling is important for understanding fundamental terrestrial processes associated with the effects of climate variability and human activities on water resources availability. However, the spatial resolution of current hydrological modeling studies is mostly constrained to a relative coarse resolution (~10–100 km) and they are therefore unable to address many of the water-related issues facing society. In this study, a high resolution (0.0625º, ~6 km) hydrological modeling for China was developed based on the Variable Infiltration Capacity (VIC) model, spanning the period from January of 1970 to June of 2016. Distinct from other modeling studies, the parameters in the VIC model were updated using newly developed soil and vegetation datasets, and an effective parameter estimation scheme was used to transfer parameters from gauged to ungauged basins. Simulated runoff, evapotranspiration (ET), and soil moisture (SM) were extensively evaluated using in-situ observations, which indicated that there was a great improvement due to the updated model parameters. The spatial and temporal distributions of simulated ET and SM were also consistent with remote sensing retrievals. Moreover, this high-resolution modeling is capable of capturing flood and drought events with respect to their timing, duration, and spatial extent. This study shows that the hydrological datasets produced from this high-resolution modeling are useful for understanding long-term climate change and water resource security. It also has great potential for coupling with the China Land Data Simulation System to achieve real-time hydrological forecasts across China.

1 Introduction

Climate change and human activities impart substantial influences on hydrological cycles and water resources, resulting in many challenges in multi-scale hydrological research (Devia et al., 2015). Water-related research has largely been reshaped by the need to solve practical problems, such as predicting floods and droughts, managing water resources, and designing water supply infrastructures at finer scales (Kirchner, 2006). As an alternative solution, high-resolution hydrological modeling is key to supporting analyses of land–atmosphere interactions, surface and subsurface interactions, water quality, and human impacts on the terrestrial water cycle (Wood et al., 2011) , and can serve as a benchmark for evaluating extreme events and for preventing record-setting disasters in advance (Lee et al., 2017). Developing a high-resolution hydrological modeling is also recognized as important for understanding the implications of climate change (Zhu and Lettenmaier, 2007) and improving the ability of scientists to narrow uncertainties and errors in water resources management (Scherer et al., 2015).

At present, hydrological modeling are usually implemented at resolutions from 0.125° to 2° latitude by longitude and with temporal resolutions from hourly to daily (Cherkauer et al., 2003; Troy et al., 2008) across different regions, such as Mexico (Zhu and Lettenmaier, 2007), Texas (Lee et al., 2017), and the Mississippi watershed (Scherer et al., 2015). China is one of the most interesting study areas for many researchers and hydrological modeling of China have also been simulated in a variety of studies (Wang et al., 2011; Wang et al., 2012; Xie et al., 2007; Zhang et al., 2014).

Hydrol. Earth Syst. Sci. Discuss., https://doi.org/10.5194/hess-2019-72
Manuscript under review for journal Hydrol. Earth Syst. Sci.
Discussion started: 13 February 2019

However, many terrestrial hydrologic and vegetative states and fluxes are typically constrained at rather coarse spatial resolutions (~10–100 km), which cannot adequately address critical scientific questions about the water cycle (Wood et al., 2011) or to describe hydrological process and water dynamics in small watershed, especially when there is a need to detect the impact of extreme events.

In recent decades, many devastating natural disasters have occurred frequently worldwide and in China due to global climate change (Mo et al., 2016; Piao et al., 2010; Xu et al., 2015). The intensification of droughts and floods is having a critical negative impact (i.e., economic losses, agricultural destruction) in China (Zhang et al., 2015). Therefore, high-resolution hydrological modeling in China is urgently needed to identify and monitor the underlying processes and intensities of hydrological extremes (Dong et al., 2011) and to reflect the regional details of climate change patterns (Zhang et al., 2006).

However, there are disadvantages and difficulties in developing high-resolution hydrological modeling in China with respect to meteorological forcings, soil and vegetation datasets, and model evaluation. First, meteorological forcing data hold substantial uncertainties, especially for high-resolution modeling, because ground-based observation stations are limited in China. Only ~750 meteorological stations for collecting data (which may be combined with remote sensing datasets) have been commonly used to generate different resolutions of forcing data (Xu et al., 2015; Zhai et al., 2005; Zhang et al., 2014), and these datasets are only suitable for modeling at coarse resolutions (> 10 km) rather than at high-resolutions. Second, estimating model parameters presents a great challenge because the climate, soil, and land cover conditions are highly heterogeneous over the 9.6 million km^2 area of China (Zhai et al., 2005). Third, ground-based hydrological stations are extremely scarce in most basins, and hydrological datasets are insufficient for model calibration and validation. Thus, in many studies, model parameters have only be calibrated using limited streamflow data, while evapotranspiration (ET) and soil moisture (SM) states have not been well evaluated (Jiao et al., 2017; Scherer et al., 2015). Finally, remote sensing (RS) data can serve as hydrological model inputs; however, RS data have not been fully combined with hydrological modeling, although they have the potential to improve model performance (Wu et al., 2014).

In this study, we attempt to develop a high-resolution hydrological modeling framework for China at the spatial resolution of 0.0625° (~6 km). The framework is based on a land surface hydrological model, (i.e., the Variable Infiltration Capacity (VIC)) (Liang, 1994, 1996). The features of this framework include: (1) it is driven by meteorological forcing data that were generated based on data from relatively high-density ground-based stations (2481 stations), nearly tripling the number of meteorological stations when compared with other studies (Pan et al., 2012; Xie et al., 2007; Zhang et al., 2014); (2) soil parameters of the VIC were updated based on a newly developed soil dataset for China, which provides an improved representation of hydrological and biogeochemical characteristics (Dai et al., 2013; Shangguan et al., 2013); (3) an effective scheme was employed to estimate model parameters for ungauged basins; (4) the simulated runoff, ET, and SM were extensively evaluated using ground-based measurements and RS data products.

This high-resolution modeling framework has attractive applications and potential extensions. The simulated hydrological flux and state variables are useful for understanding long-term climatic changes and water resource security at various scales. Additionally, these simulated variables, benefiting from the high resolution of the modeling, can provide more detailed information for detecting drought and flood events at the regional scale. Furthermore, the framework can be extended to couple with the China Land Data Simulation System (CLDAS), which provides real-time meteorological inputs and SM conditions at the same resolution (0.0625°) (Shi et al., 2011). This hydrological modeling, driven by high-quality and real-time inputs from CLDAS, may improve the accuracy of results and estimate real-time hydrological processes.

In the next section we describe the structure of the VIC model, including its inputs data and parameters. The method of calibration and transfer parameters is also presented. In section 3, we describe the evaluation of model performance over China and the application of the modeling on extreme events. We discuss its reliability, and potential and limitation in section 4, and in section 5 we present our conclusions and thoughts on future directions.

2. Data and methods

2.1 Hydrological model

The VIC model is a distributed and physically based model that solves for the surface energy and water balance (Liang, 1994, 1996). Variable Infiltration Capacity model

Hydrol. Earth Syst. Sci. Discuss., https://doi.org/10.5194/hess-2019-72
Manuscript under review for journal Hydrol. Earth Syst. Sci.
Discussion started: 13 February 2019

simulates SM, ET, snow pack, surface runoff, baseflow, and other hydrological variables in daily or sub-daily time steps. Each grid cell is partitioned into multiple vegetation types, and the soil column has three soil layers, where each layer characterizes the dynamic response of the soil to climatic conditions. The VIC model characterizes multiple land cover types, with one type of bare soil. Each vegetation type has a leaf area index (LAI), minimum stomatal resistance, roughness length, displacement length, and relative fraction of the root (Umair et al., 2018).

This model is selected for use in this study due to three main advantages: (1) a simple conceptual rainfall–runoff model is used that allows the spatial representation of gridded topography, infiltration rate, soil properties, climate variables, and land covers, which are important factors in modeling runoff under spatially heterogeneous conditions (Tesemma et al., 2015); (2) both infiltration and saturation excess runoff generation mechanisms are considered in the model, making it suitable for application to both arid and humid regions; (3) simulations of snow and frozen soil processes, which are necessary for the Tibet Plateau, can be performed. Finally, the VIC model has also been shown to represent land surface hydrologic processes well in numerous studies (Luo et al., 2013; Wu et al., 2014), and has been used from global (Bart Nijssen et al., 2001; Haddeland et al., 2007) to river basin scales (Liang and Xie, 2001) to assess water resources, land–atmosphere interactions, and overall hydrological budgets.

2.2 Data for model inputs

2.2.1 Meteorological forcing data

The VIC model is driven by historical meteorological forcing, including precipitation (mm), minimum and maximum temperature (°C), and wind speed (m/s). We ran the model in daily time steps from 1970–2016 in a water-balance mode. All of the forcing data were produced by interpolating ground-based observations from 2481 meteorological stations in China (Fig. 1a), which were obtained from the China Meteorological Administration (CMA). These data were interpolated into a gridded dataset (at a resolution of 0.0625º × 0.0625º) by a linear interpolation method using an inverse squared distance between the stations. At least five stations around the target grid were searched to conduct this interpolation. A lapse rate of $-6.5°C\ km^{-1}$ with respect to the elevation difference between the station and the target grid was used to reflect the decrease in temperature with increasing elevation. The same interpolation method for generating gridded forcing data has been successfully applied in previous VIC simulations(Xie and Cui, 2011; Xie et al., 2015; Xie et al., 2007).

2.2.2 Vegetation dataset

Vegetation data needed for VIC simulations included land cover (LC) types and associated vegetation parameters. Details of the LC types were originally created by merging a number of Land Satellite Thematic Mapper (Landsat TM) images (Liu et al., 2010), with a spatial resolution of 1 km. There were 12 types of LC distributed across China. Based on these LC types, the fractional area of each vegetation type in a grid cell was calculated.

The parameters for each type of vegetation (e.g., the architectural resistance) are available from ftp://ftp.hydro.washington.edu/pub/HYDRO/models/VIC/Veg/veg_lib, except for the LAI. The LAI reflects the amount of available leaf material, and thus, represents the canopy density and growth of vegetation, and influences the ET process (Hanes and Schwartz, 2010). Monthly LAI data at a spatial resolution of 0.1º (~8 km) were obtained from the Advanced Very High Resolution Radiometer (AVHRR) satellites acquired between January of 1982 and December of 2006, and they were derived from an 8-km composited AVHRR Normalized Difference Vegetation Index (NDVI) (Strahler et al., 1999). Hence, based on the LC maps and the LAI data, vegetation parameters were generated for use in the VIC simulations.

2.2.3 Soil dataset

Soil datasets define the soil physical and chemical properties of grid cells. In this study, detailed information on the physical and chemical properties of soils were obtained based on a 30 × 30 arc-second-resolution soil characteristics dataset (Dai et al., 2013; Shangguan et al., 2013) derived by using the 1:1,000,000 Soil Map of China and 8595 representative soil profiles.

This dataset is specifically suitable for land surface modeling, so it can be incorporated into hydrological models to better represent the role of soils in hydrological and biogeochemical cycles in China. Four influential soil parameters (i.e., field capacity, wilting point, saturated hydraulic conductivity, and bulk density) for each of the three layers were obtained from the soil dataset (Dai et al., 2013; Shangguan et al., 2013) and then applied to the 0.0625º grid in this study. The other soil parameters, such as the thermal damping depth, bubbling pressure, surface roughness of bare soil, and snowpack were prescribed according to the Food and Agriculture Organization (FAO) of the United Nations (UN) dataset, which has been successfully used by Nijssen et al.

Hydrol. Earth Syst. Sci. Discuss., https://doi.org/10.5194/hess-2019-72
Manuscript under review for journal Hydrol. Earth Syst. Sci.
Discussion started: 13 February 2019

(2000); Nijssen et al. (1999).

2.3 Data for model evaluation

2.3.1 Streamflow

The VIC model was first calibrated and validated using streamflow data. We obtained streamflow data for 29 stations from the Annual Hydrological Report for P.R. China (Fig. 1b). These stations are situated at the outlets of 29 sub-catchments that have different climatic and LC conditions. The data were partitioned into two groups, 20 stations of data were used for calibration and the remaining 9 were then used for model validation.

2.3.2 Evapotranspiration (ET)

Evapotranspiration is the second largest term in the global land surface water budget (Bohn and Vivoni, 2016), and it was evaluated in our model by using ground-based observations and an RS product. Ground-based observations of ET were obtained at 33 covariance tower stations (Fig. 1b). The RS ET product was from the Global Land Surface Satellite (GLASS) and, which merges multiple sources of RS data to achieve reliable ET estimates (Liang et al., 2013; Yao et al., 2015; Yao et al., 2014; Zhao et al., 2013), and thus it was used to spatially evaluate the VIC-simulated ET. Moreover, the GLASS ET was approximately equal in spatial resolution (0.05º) to the model in this study, and was therefore applicable to the evaluation of ET.

2.3.3 Soil moisture (SM)

Soil moisture plays an important role in the terrestrial hydrological cycle, and it also connects agricultural drought events. Therefore, the validation of SM was also performed in this study. Soil moisture data from 45 in situ stations across China (Fig. 1b) obtained from the CMA were for this assessment. To guarantee the reliability of the validation results, we selected stations that were close to the center of a target grid and covered a long measurement period. Except for the ground-based observation data, the RS SM data are available from the European Space Agency Water Cycle Multimission Observation Strategy and Climate Change Initiative projects (ESA-CCI SM). The ESA-CCI product provides relatively consistent and reliable information for SM worldwide (Qiu et al., 2016) and has been successfully validated by many researchers (Dorigo et al., 2015; Wang et al., 2016).

Hydrol. Earth Syst. Sci. Discuss., https://doi.org/10.5194/hess-2019-72
Manuscript under review for journal Hydrol. Earth Syst. Sci.
Discussion started: 13 February 2019

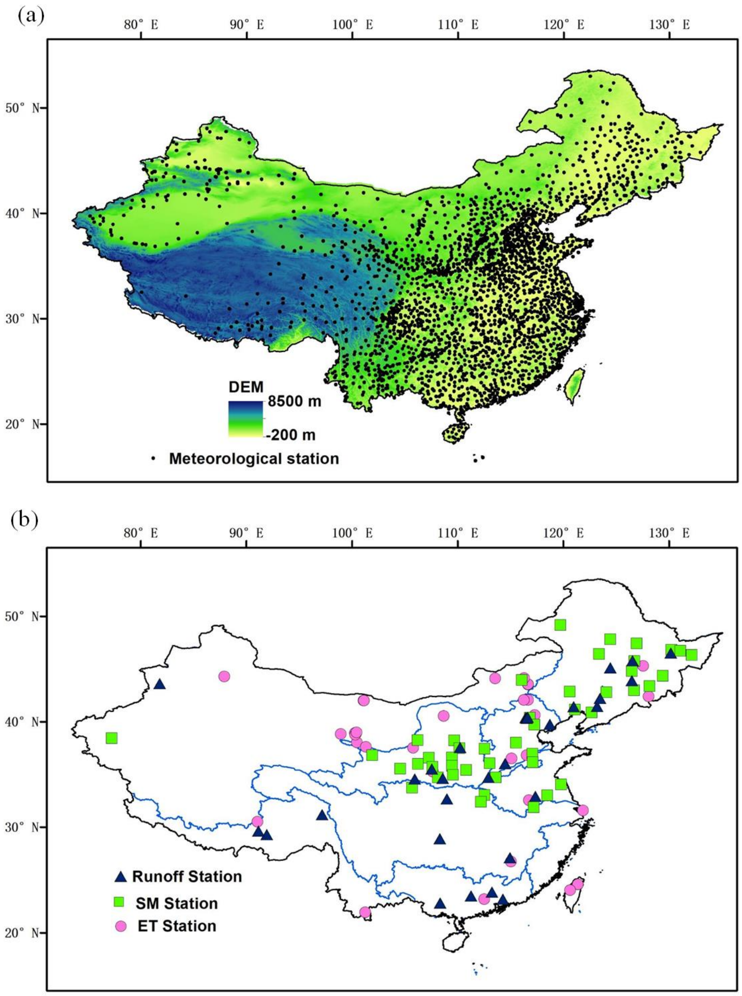

Figure 1: Distribution of (a) meteorological stations and (b) in situ runoff stations, SM and ET stations.

2.4 Parameter calibration and transfer scheme

2.4.1 Parameter calibration

After all of the necessary input data for the model were collected and prepared, the VIC model was calibrated for the selected 20 basins and validated for the 9 basins located in different climate zones (Fig. 1). Most basins were minimally affected by human

Hydrol. Earth Syst. Sci. Discuss., https://doi.org/10.5194/hess-2019-72
Manuscript under review for journal Hydrol. Earth Syst. Sci.
Discussion started: 13 February 2019

Hydrology and Earth System Sciences
Open Access
Discussions

activities, such as water extraction, irrigation, and water management. Seven of the most sensitive VIC model parameters were targeted for calibration in each basin separately, including the infiltration curve, b, the depths of the three soil layers (d_1, d_2, d_3), the maximum velocity of the baseflow, D_{smax}, the fraction of the maximum baseflow velocity, D_s, and the fraction of the baseflow of the maximum SM where non-linear baseflow occurs, W_s. The parameters D_{smax}, D_s, W_s, and d_3 are influential for runoff and for early season SM and ET since they govern water infiltration and baseflow generation (Bennett et al., 2018). The initial values of these sensitive parameters were obtained from Zhang et al. (2014) at a 0.25º resolution and then were directly downscaled to a 0.0625º resolution. The calibration involved setting an identical parameter set for each basin to find the best combination of the seven parameters. It was performed via a trial and error procedure to match the simulations with the hydrograph observations.

Three metrics were used to evaluate model performance: (1) the correlation coefficient (R), (2) the Nash-Sutcliffe efficiency (NSE), and (3) the relative error (bias; %) between observations and simulations.

$$\mathrm{NSE} = 1 - \frac{\Sigma\left(Q_{i,obs} - Q_{i,sim}\right)^2}{\Sigma\left(Q_{i,obs} - \overline{Q_{obs}}\right)^2} \quad (1)$$

$$\mathrm{Bias}(\%) = \frac{\left(\overline{Q_{sim}} - \overline{Q_{obs}}\right)}{\overline{Q_{obs}}} \times 100\% \quad (2)$$

In Eqs. 1 and 2, $Q_{i,obs}$ is the observed flow in the i month, $Q_{i,sim}$ is the respective ith simulated flow from the model, and $\overline{Q_{sim}}$ and $\overline{Q_{obs}}$ are the observed and simulated mean annual discharges for the calibration period, respectively.

For each grid cell in the calibrated basins, an adjustment factor (*Adj_factor*) can be defined as:

$$Adj\_factor = \frac{PAR_{final}}{PAR_{initial}} \quad (3),$$

where PAR_{final} and $PAR_{initial}$ are the final and the initial estimates of the parameter, respectively. Based on this adjustment factor, the estimates of parameters in the calibrated basins were transferred to the uncalibrated basins.

2.4.2 Parameter transfer

The area of China was divided into nine large river basins (Fig. 2) according to topographic and LC conditions. As the VIC model parameters are closely related to physical and climatic characteristics of basin properties, such as LC and meteorological factors, we overlaid the river basins with climate zones to define a climatic similarity, as described by Xie et al. (2007). Based on the climatic similarity and the adjustment factor described in Sect. 2.4.1, the estimated parameters in calibrated basins were transferred to the uncalibrated basins. The 20 independent, calibrated basins were located in different climate zones and designed to estimate the parameters in their uncalibrated, climate-related areas. Seven climatic zones in China, as defined based on the Köppen classification criteria (Kottek et al., 2006), are shown in Table 1 and Fig. 2. The parameter transfer strategy has been successfully used by Xie et al. (2007), and it is briefly described as follows:

(1) The adjustment factors in each calibrated basin were used to adjust parameters in uncalibrated basins;

(2) The rainy climate zone was further divided into three parts according to basins of the Huai River, Yangtze River, and Pearl River, as C1, C2, and C3, respectively;

Hydrol. Earth Syst. Sci. Discuss., https://doi.org/10.5194/hess-2019-72
Manuscript under review for journal Hydrol. Earth Syst. Sci.
Discussion started: 13 February 2019

Hydrology and Earth System Sciences
Discussions
Open Access

(3) The tropical climate zone has similar climatic characteristics to the Pearl River basin. Therefore, the parameters for the tropical climate zone were set to the same adjustment values as C3;

(4) Parameters of southeastern basins were used as the equivalent multiple as the Yangtze River basin C2;

(5) The Dc climate zones covers two different regions in northeastern and southeastern China (Dc east and Dc west). Therefore, the parameters in Dc east and Dc west were adjusted using the same multiples from the related Da and E zones, respectively.

Table 1: Classification of Köppen climate zones.

Climate zones	Description	Criterion
A	Equatorial climate	Tmin ≥ +18 ℃
Bk	Dry, cold climate	Tann < +18 ℃
C	Rainy, midlatitude climate	−3 ℃< Tmin < +18 ℃
Da	Continental climate with hot summer	Tmax ≥ +22 ℃
Db	Continental climate with cool summer	Tmin ≤−3 ℃ not (a) and at least 4 Tmon ≥ +10 ℃
Dc	Continental climate with short cool summer	not (Bk) and Tmin > −38 ℃
E	Polar climate	Tmax < +10 ℃

Hydrol. Earth Syst. Sci. Discuss., https://doi.org/10.5194/hess-2019-72
Manuscript under review for journal Hydrol. Earth Syst. Sci.
Discussion started: 13 February 2019

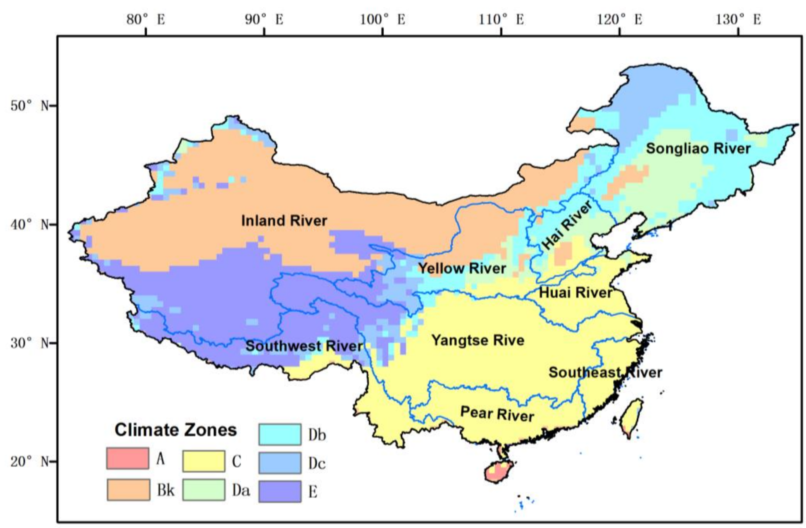

Figure 2: River basins and climate zones in China.

3. Results

3.1 Runoff calibration and validation

To highlight the advantages of updating soil model parameters, we conducted two simulations: one using the original soil parameters, which were directly downscaled from a 0.25° resolution, and the other employing the updated soil parameters with parameter calibration. Figure 3 presents the monthly discharge of the simulations from the original and calibrated parameters and observations over 9 river basins, which were chosen to be regionally representative and distributed among diverse climates. The model performance was considerably better when using the calibrated parameters rather than the initial parameters (Sect. 2.4.1). For most basins, the simulations with defaults parameters tended to have higher discharges, especially overestimating the peak flow during summer, such as in Phujym, Jilin, Heishiguan, and Tsuuang. In contrast, the calibration was able to successfully avoid the overestimation of peak flow. However, for the Shetang, Maojiahe, and Tsyamusy basins, which have little rainfall and runoff, the initial parameters do not match the observations well at first during the low-flow seasons, but this phenomenon changed after parameter calibration. Overall, the comparisons revealed that the runoff dynamics were well captured after calibration, and consequently the calibrated results were improved relative to the original VIC simulations.

In Table 2, the model performances are listed for each basin after calibration and validation. The correlation coefficient, NSE, and bias were used to evaluate the simulations against observations. Most of the calibrated basins had high R and NSE values of more than 0.70. The relative bias presented here is generally within 20%. The simulations of basins located in southern China (e.g., C1, C2, and C3), which usually receive abundant rainfall and experience substantial runoff throughout the entire year, tended to have better agreements with observations than those in northern China (e.g., Da, Db, and Bk). In general, the calibration improved the results in all instances, although in some basins, such as Dingjiagou and Phujym, the results were still unsatisfactory. A possible reason for such a discrepancy is that the VIC model is unable to capture the impact of human activities, such as reservoir regulations.

The streamflow values simulated using the parameters sets through the parameter transfer scheme were validated over 9 basins based on the observations. Compared with the calibration process, six validation basins covering two climate zones, such as Da and Db, were used to examine the performance of the parameter transfer approach. Overall, the validation results (Table 2) were consistent with the calibration statistics.

Hydrol. Earth Syst. Sci. Discuss., https://doi.org/10.5194/hess-2019-72
Manuscript under review for journal Hydrol. Earth Syst. Sci.
Discussion started: 13 February 2019

The *R*, NSE, and bias values for the validation period ranged from ~0.65–0.91, ~0.31–0.87, and ~4.29–40.5%, respectively. The Zhangjiashan Basin had a relatively high bias, mainly because there were only two years of observation data available for validation. The best performance was found in the Hengshi Basin, while the worst was in the Chiling Basin.

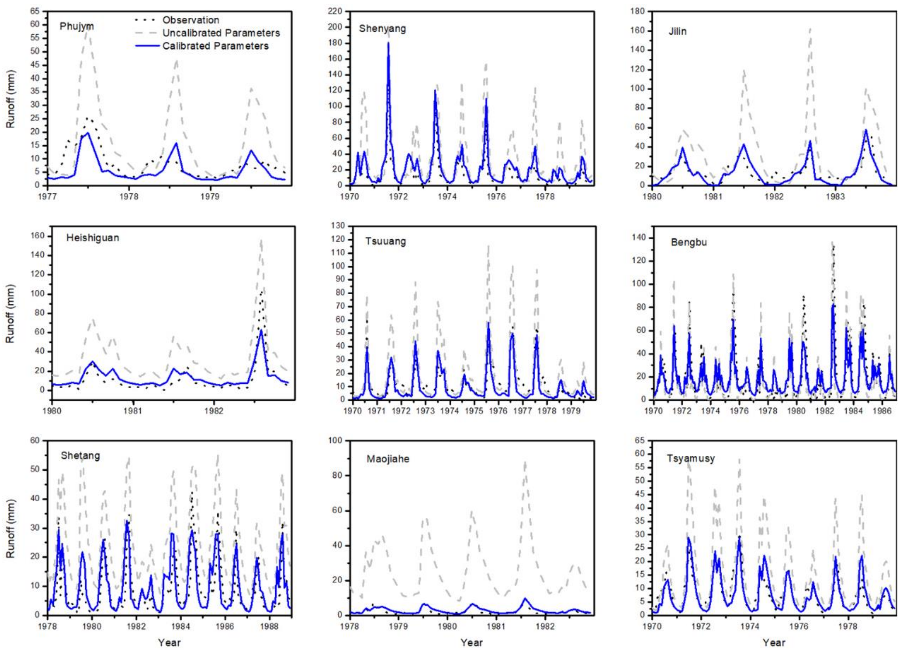

Figure 3: Monthly discharges for some calibrated basins. The stippled lines are observations, dashed lines are simulations from uncalibrated parameters, and the solid lines are simulations from calibrated parameters.

Table 2: Statistics of calibrated and validated monthly flows.

Location	Latitude	Longitude	Climate Zone	Period	R	NSE	Bias

Hydrol. Earth Syst. Sci. Discuss., https://doi.org/10.5194/hess-2019-72
Manuscript under review for journal Hydrol. Earth Syst. Sci.
Discussion started: 13 February 2019

Calibration							
Yamadu	43.62	81.8	Bk	2006-2008	0.91	0.59	7.59%
Dingjiagou	37.55	110.25	Bk	1970-1986	0.47	0.26	−20.70%
Bengbu	32.93	117.38	C1	1970-1986	0.82	0.65	−2.78%
Tsuuang	36.03	114.52	C1	1970-1979	0.89	0.76	−18.50%
Heishiguan	34.71	112.93	C1	1980-1982	0.91	0.72	25.40%
Jian	27.1	114.98	C2	1980-1982	0.86	0.75	−4.86%
Ankang	32.68	109.01	C2	1980-1982	0.94	0.79	37.70%
Gongtan	28.9	108.35	C2	1980-1982	0.89	0.74	−11.20%
Hoiyang	23.17	114.3	C3	1970-1982	0.92	0.74	−3.54%
Wuzhou	23.48	111.3	C3	1970-1984	0.92	0.79	12.80%
Nanning	22.8	108.36	C3	1970-1983	0.87	0.74	13.60%
Shenyang	41.46	123.24	Da	1970-1978	0.97	0.77	25.60%
Jilin	43.88	126.53	Da	1980-1983	0.85	0.56	−7.61%
Phujym	45.1	124.49	Da	1977-1979	0.68	0.26	1.23%
Tsyamusy	46.5	130.2	Db	1970-1978	0.86	0.69	−3.84%
Shetang	34.55	105.97	Db	1978-1988	0.78	0.58	12.40%
Maojiahe	35.52	107.58	Db	1978-1982	0.84	0.61	28.60%
Yangcun	29.3	91.96	E	1971-1975	0.88	0.6	−6.77%
Changdu	31.18	97.18	E	1975-1982	0.94	0.82	7.04%
Lasa	29.63	91.15	E	1973-1975	0.93	0.81	5.26%

Validation							
Zhangjiashan	34.63	108.60	Bk, Db	1980-1982	0.91	0.67	40.5%
Zhanjiafeng	40.37	116.47	Da, Db	1970-1979	0.85	0.69	4.29%
Dalinghe	41.41	121.00	Da, Db	1970-1979	0.91	0.76	−6.97%
Chiling	42.20	123.50	Da, Db	1970-1979	0.71	0.31	9.85%
Luanxian	39.73	118.75	Da, Db	1970-1983	0.91	0.79	9.69%
Haerbin	45.77	126.58	Da, Dc	1970-1983	0.78	0.51	−9.87%
Hengshi	23.85	113.27	C3	1976-1979	0.95	0.87	15.5%
Qianxinzhuang	40.32	116.55	Db	2006-2014	0.65	0.34	6.90%
Boyachang	40.40	116.65	Db	2006-2014	0.84	0.68	9.76%

3.2 ET evaluation

The root mean square error (RMSE) is a widely used measure of the differences between model and observed variations (Yin et al., 2016). In this study, the RMSE was also employed to estimate the differences between VIC model simulations and in-situ observations. The statistics of the comparison between simulations and observations are shown in Fig. 4 and Fig. 5 provides a comparison of some selected stations in the four main basins (i.e., Songliao River Basin, Hai River Basin, Yellow River Basin and Yangtse River Basin). The VIC model performed well and showed reasonable consistency at the eddy covariance tower stations with respect to daily ET, with most *R* values being greater than 0.6. The average RMSE values ranged between 0.6 mm and 3.6 mm. With respect to bias, many stations located in central China had values between

−60% and 20%. Weaker performances also occurred at a few stations mainly due to the inconsistent scales of the two datasets, as the observation dataset includes single point results, while model simulations are regionally averaged results. Therefore, the errors may result from uncertainties in the in-situ measurements themselves and from differences in the spatial scales between the model and the in situ measurements (Gruber et al., 2013). As a whole, the strong relationships between ET simulations and in-situ observations imply that they are qualitatively acceptable.

As for the spatial comparison of ET, Fig. 6 shows the seasonal changes and differences between the VIC simulated ET and the GLASS ET. The VIC simulated larger ET values in southeastern China and lower values for other areas relative to the GLASS products. The differences ranged from −2 to 2 mm/day and this may have been caused by the different temporal resolutions, which is 8 days for GLASS products. The average difference for the four seasons was only approximately –0.36 mm, and thus the VIC simulated ET was consistent with the RS estimated ET, implying an acceptable performance for the model in this study.

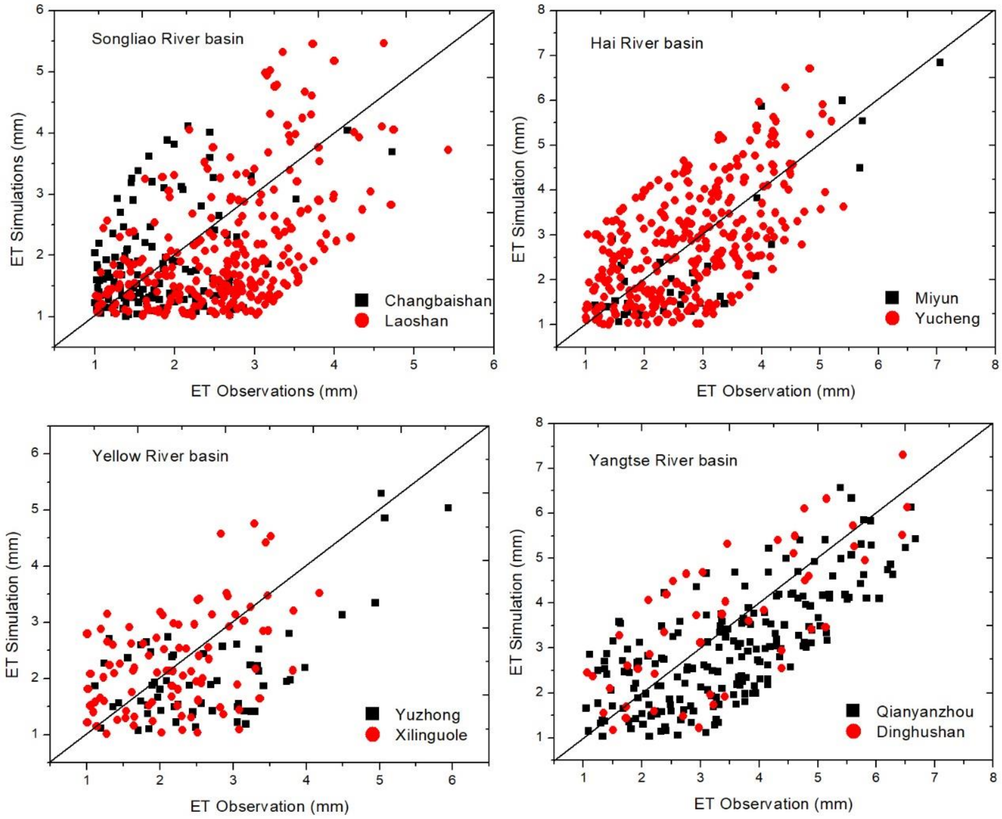

Figure 4: Comparison of ET between observations and simulations of selected stations in four basins.

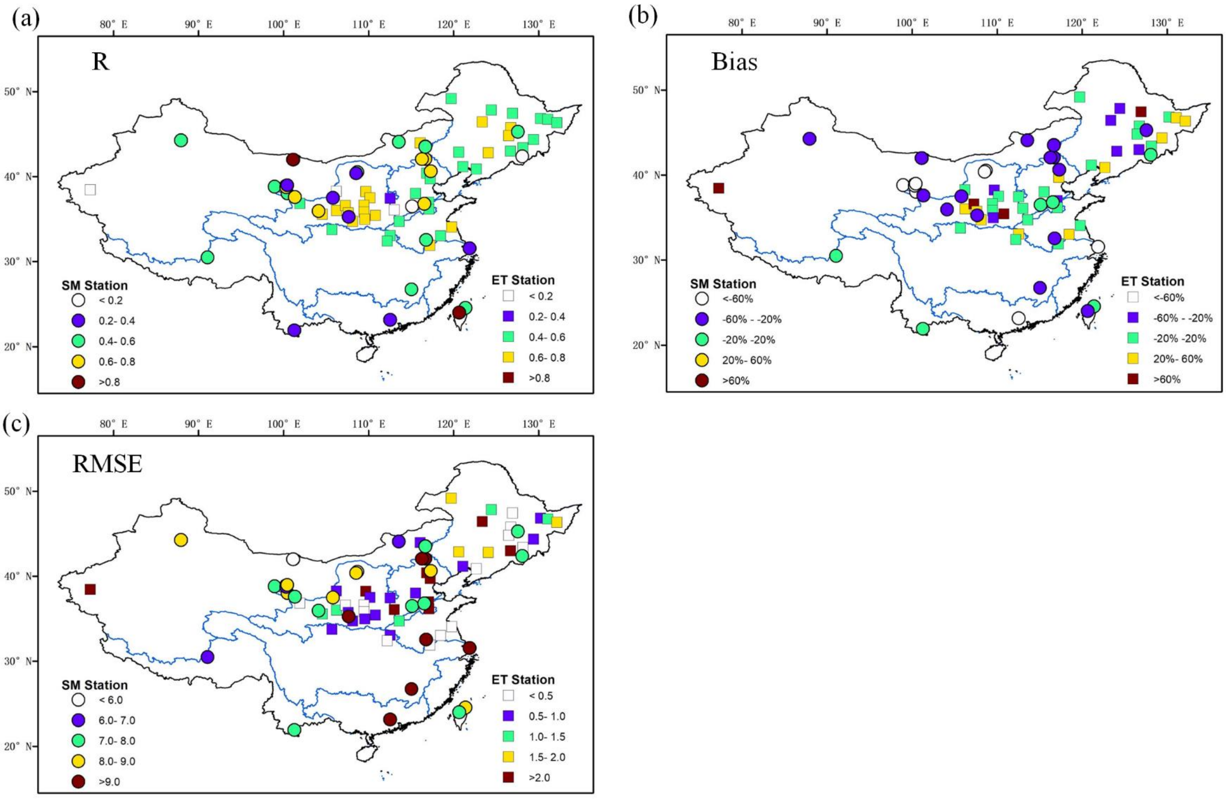

Figure 5: Spatial distribution of the correlation coefficient (*R*), bias, and RMSE between observations and simulations for ET and SM.

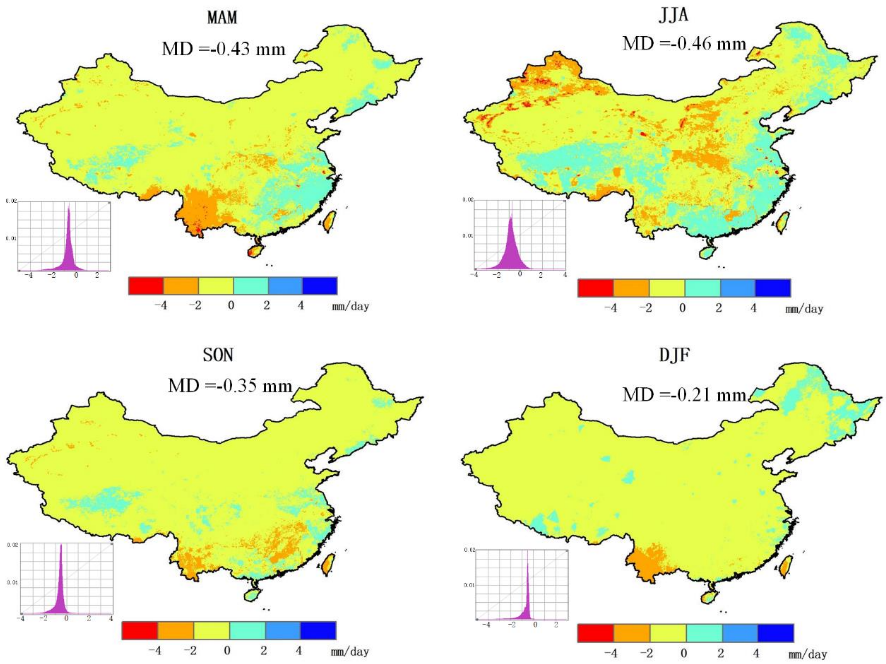

Figure 6: Seasonal differences of ET between simulation and the GLASS for, from top to bottom, spring, summer, autumn, and winter. MD is the mean differences.

3.3 SM evaluation

Figures 5 and 7 show the performance of the top 10-cm soil layer model estimates against in-situ SM observations. As shown in Fig. 5, the *R* values for most stations were higher than 0.6 and the RMSEs were less than 12 mm. There was a pattern that emerged in which stations with a high *R* values (> 0.7) usually showed considerably low RMSEs, indicating *R* and the RMSE are not independent indicators of SM. Although several comparisons showed poor results, potentially because of the differences in temporal (10 days for observations and daily for simulations) and spatial resolutions. The stations located in central China, such as the Yellow River Basin and Hai River Basin, tended to have lower biases, ranging from −20% to 20%. Meanwhile, the rural stations had larger biases, which may due to limited and/or inaccurate observation data. Overall, the comparisons of the two SM datasets demonstrated that they matched reasonably well. The ESA-CCI SM product was used to evaluate the SM results from spatial perspective. Figure 8 describes the differences between model simulations and ESA-CCI results. The important differences in winter (December–February) can be seen in southwestern China, and reached more than 10 mm. The opposite pattern appeared in summer (June–August), with high differences exhibited in southeastern China. Slight differences between simulations and the ESA-CCI product were found in spring (March–May), with high values in the Yangtze River Basin. In autumn (September–November), the southern region was covered by high differences values, which is distinctly different from northern China. Combined, these results indicate that the VIC model with properly calibrated parameters provides satisfactory simulations of runoff, ET, and SM.

Hydrol. Earth Syst. Sci. Discuss., https://doi.org/10.5194/hess-2019-72
Manuscript under review for journal Hydrol. Earth Syst. Sci.
Discussion started: 13 February 2019

Hydrology and Earth System Sciences
Open Access
Discussions

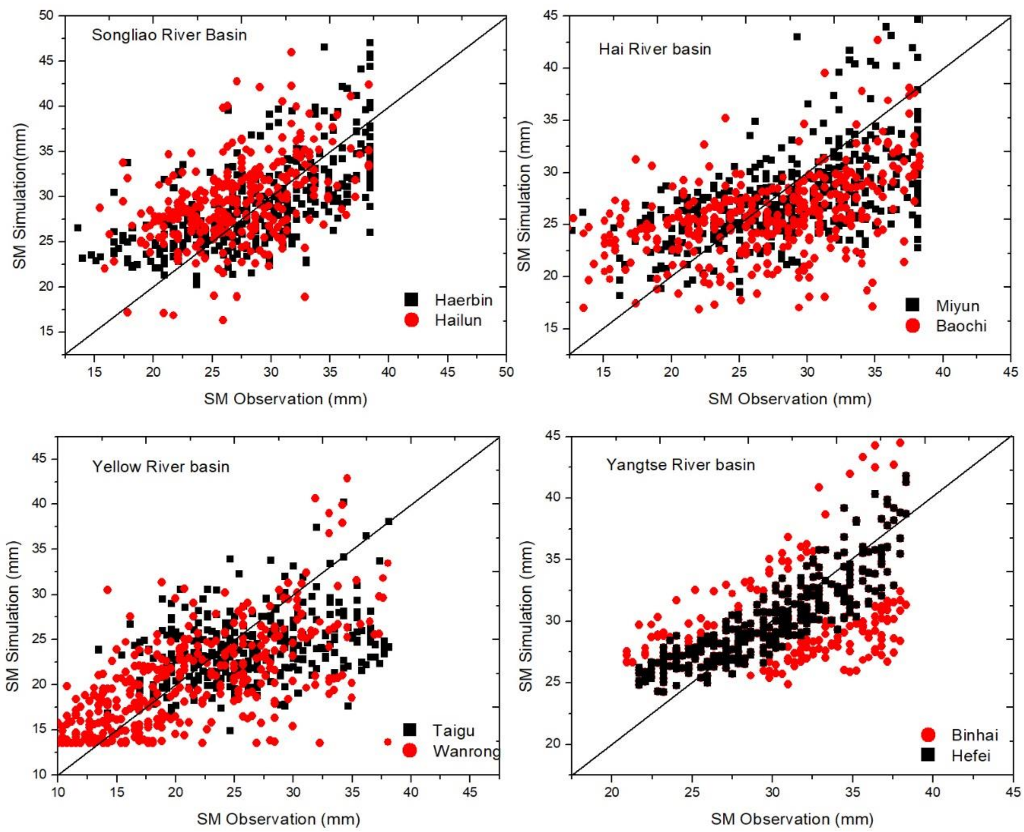

394

395 **Figure 7: Comparison between observations and simulations of selected stations**

396 **in four basins.**

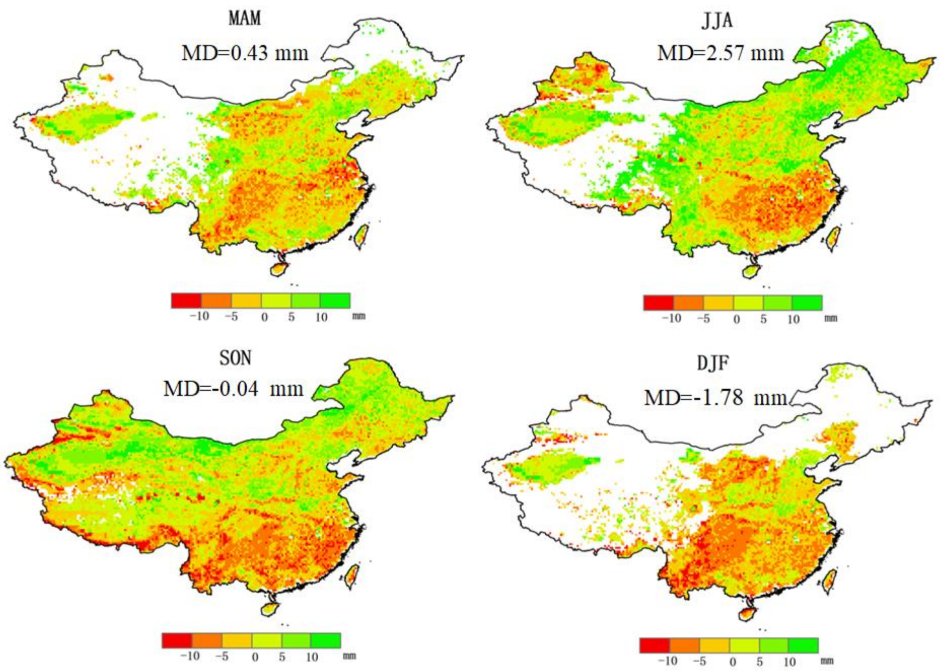

Figure 8: Seasonal distributions of differences between simulations and the ESA-CCI cases for the 0-10 cm soil layer SM. From top to bottom for: spring, summer, autumn and winter. MD is the mean differences.

3.4 Application for detection of typical extreme events

Flood and drought are the main natural disasters that occur in China, and they have become important restricting factors for the development of society, the economy, and agriculture (Zhang et al., 2016). However, the lack of high-resolution data makes identifying flash floods and droughts over short timescales (pentads or weeks) nearly impossible (Zhang et al., 2017). It is also necessary to monitor flood and drought events in small regions, especially for remote areas without sufficient and reliable observation data. Therefore, reliable, high-resolution modeling is essential for better analyzing historical and predicted extreme events and then to make informed decisions in flood and drought management. In this study, we applied the simulated 0.0625º dataset to analyze two typical extreme disasters that occurred during recent years in China and to evaluate the potential of the modeling to detect drought and flood events.

3.4.1 Beijing flood event of 2012

On July 21, 2012, the heaviest rainfall over the past six decades lashed Beijing. An area of ~16,000 km^2 and more than 1.6 million people were affected by the flood (Wang et al., 2013). A few studies have focus on the causes and patterns of this heavy rainfall (Huang et al., 2014; Liu et al., 2003), while little attention has been paid to the associated hydrological processes, such as the generation of runoff.

Here, we detected the flood coverage, which is represented by the runoff depth. According to gauge observations, the intensive rainfall area extended from southwestern Beijing to the northeastern areas (Chen et al., 2014). As shown in Fig. 9, the runoff depth presented a SE–NE zonal distribution. However, the central region of Beijing, which has the highest population and number of buildings, suffered the deepest runoff, > 100 mm/day. This may have been due to the effects of urbanization during recent years. There were four photos (Fig. 9) taken on July 21, 2012 that show the real influence of this flood event (http://www.weather.com.cn).

To further evaluate the intensity of the flood event, we analyzed the frequency distributions of precipitation and runoff (Fig. 10). The maximum precipitation was 287

Hydrol. Earth Syst. Sci. Discuss., https://doi.org/10.5194/hess-2019-72
Manuscript under review for journal Hydrol. Earth Syst. Sci.
Discussion started: 13 February 2019

mm over 24 hours, more than 50 mm of which was recognized as a rainstorm level in 76% of the area of Beijing. The mean precipitation is 103 mm on July 21, 2012. Affected by the heavy rain, the maximum runoff is 172 mm; the average runoff is 26 mm for 24 hours. It should notice that the central urban area has the highest runoff coefficient (Runoff/Precipitation) of 0.89, indicating that it will be at high flood risk during urbanization when extreme rainfall happens (Wang et al., 2013).

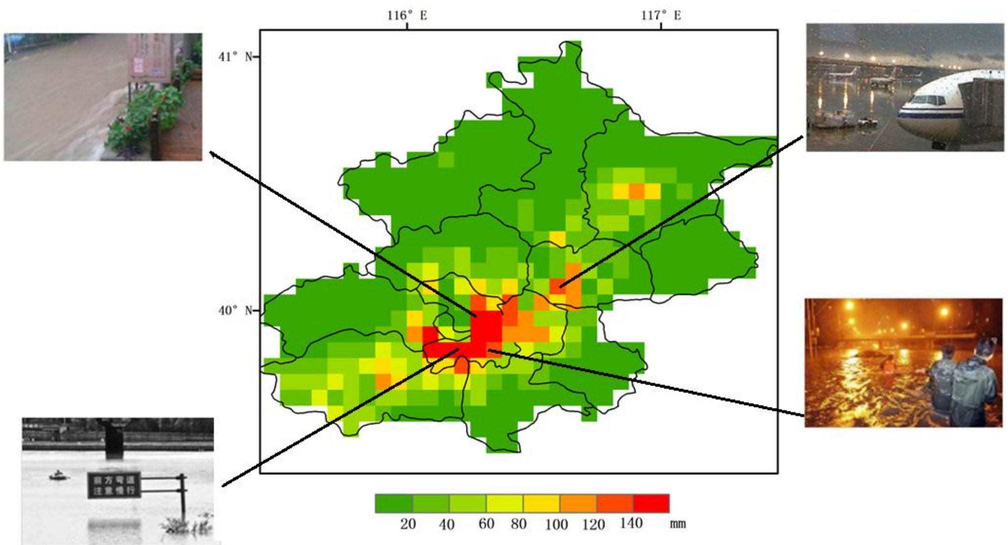

Figure 9: Simulated runoff in Beijing on July 21, 2012

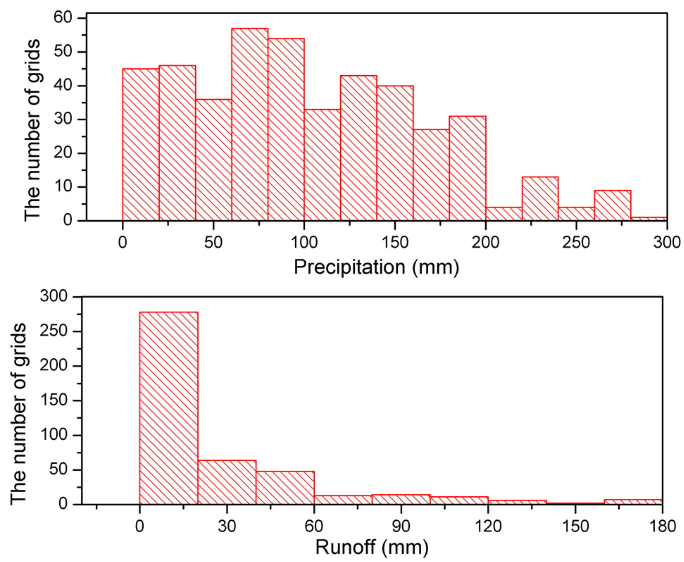

Figure 10: Statistics of the numbers of grids with different precipitation and runoff.

3.4.2 North China drought event of 2009

From 2009–2010, a large-scale severe drought struck China (Ye et al., 2012). It lasted for several months and subsequently has been considered as the most influential drought event in northern and southwestern China (Zhu et al., 2018). In August 2009, some portions of North China received only one inch of rainfall during the entire year. In August of 2009, some portions of North China had received only one inch of rainfall over the entire year.

As a result, this severe drought cost $100 million worth of losses. In this study, the VIC-simulated SM was used to assess the severity and extent of the drought, particularly focusing on agricultural drought, which was defined as a SM deficit. To emphasize the advantage of high-resolution modeling for drought detection, we conducted a coarse-resolution modeling at a 0.25º resolution that had the same sources of meteorological

Hydrol. Earth Syst. Sci. Discuss., https://doi.org/10.5194/hess-2019-72
Manuscript under review for journal Hydrol. Earth Syst. Sci.
Discussion started: 13 February 2019

forcing and soil and vegetation parameters as the 0.0625° modeling so that the only difference between the two simulations was the spatial resolution.

The simulated drought event patterns of the two simulations showed a SE–NE zonal distribution. However, differences between the simulations were obvious. The severe drought in the 0.0625° simulations extended over more areas in northwestern and southern China than in the 0.25° simulations. The Hai River Basin was selected in order to distinguish the regional differences between the two simulations. The Hai River Basin is one of the largest basins in North China, and contains a large population of 137 million people (Qin et al., 2015). It has long been identified as being sensitive to climate change and has a recorded history of decades long droughts events. As shown in Fig. 11(c) and (d), the SM anomaly shows more detailed spatial structures with the increased spatial resolution of the simulation.

In the 0.0625° simulations, drought mainly existed in the northwestern and northeastern regions, and a few southwestern areas were also affected; these results are similar to those of Wu et al. (2015) , which were based on RS data with a 1-km resolution. However, the 0.25° simulations cannot show a detailed drought distribution. Additionally, the magnitude of the SM anomaly in 0.0625° simulation results was larger than in the 0.25° results, which ranged from −10.12 mm to 10.50 mm and −7.94 mm to 4.75 mm, respectively (Fig. 11e). In the two simulations, 53.79% and 48.13% of areas were affected by drought (i.e., the percentages of the SM anomaly were less than zero), as shown in Fig. 11(f). These results indicate that the 0.0625° simulation could successfully capture detailed spatial distributions and the severity of drought events.

Hydrol. Earth Syst. Sci. Discuss., https://doi.org/10.5194/hess-2019-72
Manuscript under review for journal Hydrol. Earth Syst. Sci.
Discussion started: 13 February 2019

Based on these analyses, we also used the 0.0625º simulations to analyze agricultural drought events in the Hai River Basin over the last 46 years. Figure 12 shows the SM anomalies and durations of the agricultural droughts, which were calculated by the percentage of days with negative SM anomalies in a year from 1970 to 2015. As for the SM anomalies, ~50% of past 46 years have experienced drought events. Severe drought events occurred in 1972, the 1980s, 1999, and 2006. Moreover, there were 36 years in which the droughts had relatively long durations (i.e., they lasted more than six months), especially in 2006, when more than 75% of days had negative SM anomalies. Therefore, the Hai River Basin is a typical drought-prone region. It suffered several intensive and long-term drought events between 1980 and 1985, and in 1999 and 2006, and these findings are consistent with the conclusions of Qin et al. (2015).

Hydrol. Earth Syst. Sci. Discuss., https://doi.org/10.5194/hess-2019-72
Manuscript under review for journal Hydrol. Earth Syst. Sci.
Discussion started: 13 February 2019

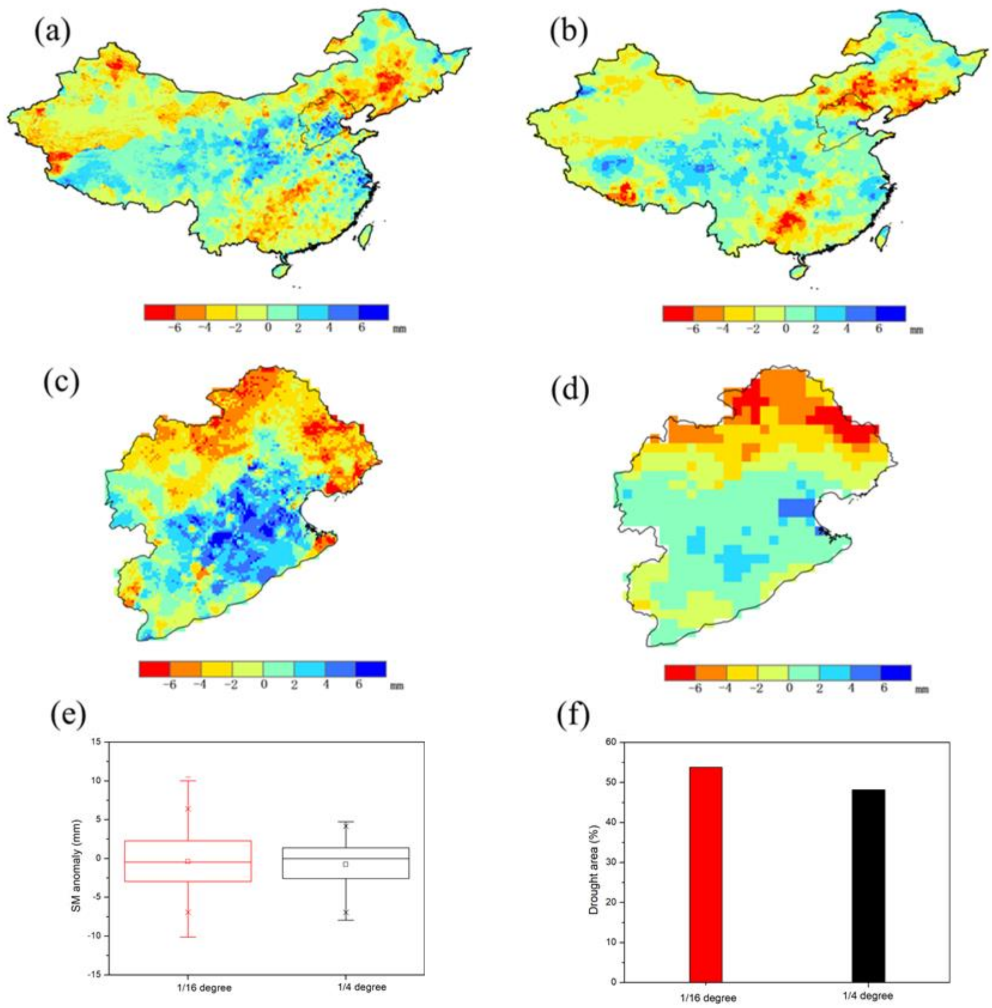

Figure 11: Soil moisture anomaly from 0.0625º simulations in (a) China and (c) the Hai River Basin, and from 0.25º simulations in (b) China and (d) the Hai River Basin. The range of the (e) SM anomaly and (f) drought area of the Hai River Basin from the two datasets are also shown.

Hydrol. Earth Syst. Sci. Discuss., https://doi.org/10.5194/hess-2019-72
Manuscript under review for journal Hydrol. Earth Syst. Sci.
Discussion started: 13 February 2019

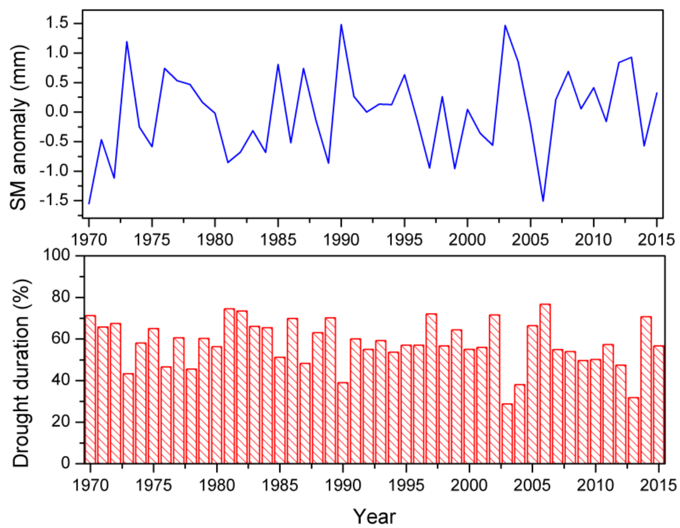

Figure 12: Monthly SM anomaly and drought duration as a percentage of each year from 1970 to 2015 in the Hai River Basin.

4. Discussion

4.1 Reliability of the modeling

In this study, we developed a framework for the high-spatial resolution hydrological modeling of runoff, ET, and SM at a 0.0625º spatial resolution across China from 1970–2016. The model is highly reliable because, with respect to the forcing data, gridded datasets were produced by interpolating station values from 2481 meteorological stations across China, in contrast to the ~700 stations that have been commonly used in many studies of China, such as that presented in the China Regional Surface Meteorological Feature Dataset (CMFD). Meanwhile, high intensity station datasets generally cover short periods of time, such as the CLDAS, which covered 2008–2016. As for modeling process, a combination of climatic zones and river basin methodologies was used to transfer the VIC parameters to uncalibrated areas. Soil

Hydrol. Earth Syst. Sci. Discuss., https://doi.org/10.5194/hess-2019-72
Manuscript under review for journal Hydrol. Earth Syst. Sci.
Discussion started: 13 February 2019

parameters, which are the most essential parameters of the VIC model, were adopted from the newly released soil datasets of Dai et al. (2013) and Shangguan et al. (2013) to improve the accuracy of hydrological modeling in our study. For model validation, some previous studies have only validated runoff results using in-situ data (Lee et al., 2017; Xie et al., 2007; Zhu and Lettenmaier, 2007), which may not guarantee the reliability for other hydrological processes, such as ET and SM. In contrast, more ground observations and RS data were used to validate simulations of runoff, ET, and SM in our study.

Therefore, this high-quality, high-spatial resolution hydrological modeling could be extended for relevant applications, such as detecting extreme events. As shown in Sect. 3.4, the simulations were capable of capturing detailed changes and providing reliable information when drought and flood events occurred.

4.2 Potential extension with China Land Data Simulation System (CLDAS) and remote sensing (RS) data

The CLDAS is a system that produces high-quality metrological forcing and SM conditions over China at a 0.0625º resolution and in hourly time steps (Shi et al., 2011). Three land surface models are included in the current version of the CLDAS-V2.0 (i.e. CLM3.5, Noah-MP, and CoLM). In terms of the Global Land Data Assimilation System (GLDAS) (Rodell et al., 2004) and the National Land Data Assimilation System (NLDAS) (Mitchell, 2004), the VIC model is considered to fully simulate hydrological processes.

In this study, the developed hydrological modeling framework based on VIC had the same resolution as the CLDAS, and it was easy to couple with the CLDAS. Therefore, this study provided an opportunity for the CLDAS to be combined with hydrological modeling to better enhance its services.

Based on the high-quality and high-density drivers from the CLDAS, the simulation of the VIC model could be applied to real-time hydrological process estimation across China, and then offer an effective guide to detecting flood and drought events. Furthermore, the RS data, such as LAI, albedo, and shortwave radiation, also could be merged into the VIC, which may improve modeling results by considering the energy balance.

4.3 Limitations

As shown in Sect. 3, the hydrological simulations were extensively validated with in situ observations and RS data. However, with the exception of two stations, all of the streamflow stations only had data records for the periods before 1990. The ET and SM observations stations were mostly distributed in North China. Additionally, we calibrated the most sensitive seven parameters of the VIC model (b, d_1, d_2, d_3, D_{smax}, D_s, and W_s), while the other parameters were not calibrated. For example, the wintertime LAI and canopy fraction has a strong influence on variations in the snow water equivalent (Bennett et al., 2018). Therefore, further efforts are needed to improve model parameters uncertainties and the accuracy and application of RS products, and to enhance the support of ground-based observation networks.

This study improved the spatial resolution of hydrological modeling to ~6 km across China, which is just one step toward further increasing the resolution. The modeling

Hydrol. Earth Syst. Sci. Discuss., https://doi.org/10.5194/hess-2019-72
Manuscript under review for journal Hydrol. Earth Syst. Sci.
Discussion started: 13 February 2019

needs to be improved to reach a so-called hyper-resolution (~1 km or finer), which is one of the "grand challenges" in current hydrological research (Wood et al., 2011). Moreover, as hydrological processes generally evolve over various temporal scales, from minute to daily time steps, future studies should also increase the evaluation of temporal resolutions simultaneously (Melsen et al., 2016). However, the modeling in our study was conducted roughly, at a daily time step, alone due to the limitations of the forcing data. Hourly or smaller time step data can capture more detailed processes, such as flash floods, infiltration, and pore flow (Blöschl and Sivapalan, 1995). Furthermore, the achievement of high-spatial and temporal-resolution modeling not only requires the resolution to increase, but also involves the development of hydrological models to consider hydrological processes that are consistent with such high resolutions, including lateral groundwater flow (Zeng et al., 2018; Zeng et al., 2016) and efficient runoff routing algorithms (Li et al., 2013; Meng et al., 2017; Wen et al., 2012; Wu et al., 2014).

5. Conclusion

In order to address the fundamental questions associated with the effects of environmental changes across various scales, we developed a high-resolution (0.0625º) hydrological modeling for China using the VIC model over the period from 1970–June 2016.

The modeled runoff, ET, and SM were fully calibrated and validated against the data from in-situ stations and RS. The modeled runoff results were significantly improved after parameter calibration and transfer using a combination of climatic zones and river

Hydrol. Earth Syst. Sci. Discuss., https://doi.org/10.5194/hess-2019-72
Manuscript under review for journal Hydrol. Earth Syst. Sci.
Discussion started: 13 February 2019

basin methodologies. Additionally, the *R* and NSE values of most calibrated and validated basins were greater than 0.70, and the relative bias was generally below 20%. The simulations of humid regions, such as the Yangtze River Basin, tended agree better with observations than those of arid regions. Furthermore, ET and SM simulations were also validated against ground observations and RS products. The *R* and RMSE values for ET and SM were quite acceptable. The simulated ET and SM and the RS products (e.g., GLASS, ESA-CCI) were consistent across spatial and temporal distributions. Therefore, the hydrological modeling is capable of capturing the hydrological processes at such a high resolutions, and can provide reliable estimates of land surface hydrological conditions in China.

Several important implications emerge from our work. For example, this implementation has a higher spatial resolution and generally improved performance relative to earlier model results (Lee et al., 2017; Zhang et al., 2014; Zhu and Lettenmaier, 2007). The increased spatial resolution improves the ability of the modeling to represent topographic effects and resolve smaller watersheds, and hence provide information relevant to local water management concerns, such as on drought and flood events.

Consequently, this is the first time that hydrological states and fluxes at a 0.0625° spatial resolution have been produced for China, and they are freely available to analyze multi-scale hydrological, ecological, and meteorological interactions and initial conditions. Additional efforts will be needed to improve the hydrological modeling by using more detailed model inputs and advanced parameter calibration techniques. Moreover, there is great potential for the extension of our modeling results with CLDAS and RS data to improve high-resolution modeling applications.

Acknowledgements

This study was supported by grants from the National Key Research and Development Program of China (NO.2016YFA0600103, No. 2016YFC0401404) and the National Natural Science Foundation of China (No. 41471019).

References**:**

Bart Nijssen, Reiner Schnur, and Lettenmaier, D. P.: Global Retrospective Estimation of Soil Moisture Using the Variable Infiltration Capacity Land Surface Model, 1980–93, Journal of Climate, 14, 1790-1808, 2001.

Bennett, K. E., Urrego Blanco, J. R., Jonko, A., Bohn, T. J., Atchley, A. L., Urban, N. M., and Middleton, R. S.: Global Sensitivity of Simulated Water Balance Indicators Under Future Climate Change in the Colorado Basin, Water Resources Research, 54, 132-149, 2018.

Blöschl, G. and Sivapalan, M.: Scale issues in hydrological modelling: a review, Hydrological Processes, 9, 1995.

Bohn, T. J. and Vivoni, E. R.: Process-based characterization of evapotranspiration sources over the North American monsoon region, Water Resources Research, 52, 358-384, 2016.

Chen, S., Huijuan Liu, Yalei You, Esther Mullens, Junjun Hu, Ye Yuan, Mengyu Huang, Li He, Yongming Luo, Xingji Zeng, Guoqiang Tang, and Hong, Y.: Evaluation of High-Resolution Precipitation Estimates from Satellites during July 2012 Beijing Flood Event Using Dense Rain Gauge Observations, Plos One, 9, 2014.

Cherkauer, K. A., Bowling, L. C., and Lettenmaier, D. P.: Variable infiltration capacity cold land process model updates, Global and Planetary Change, 38, 151-159, 2003.

Dai, Y., Shangguan, W., Duan, Q., Liu, B., Fu, S., and Niu, G.: Development of a China Dataset of Soil Hydraulic Parameters Using Pedotransfer Functions for Land Surface Modeling, Journal of Hydrometeorology, 14, 869-887, 2013.

Devia, G. K., Ganasri, B. P., and Dwarakish, G. S.: A Review on Hydrological Models, Aquatic Procedia, 4, 1001-1007, 2015.

Dong, X., Xi, B., Kennedy, A., Feng, Z., Entin, J. K., Houser, P. R., Schiffer, R. A., L'Ecuyer, T., Olson, W. S., Hsu, K.-l., Liu, W. T., Lin, B., Deng, Y., and Jiang, T.: Investigation of the 2006 drought and 2007 flood extremes at the Southern Great Plains through an integrative analysis of observations, Journal of Geophysical Research, 116, 2011.

Dorigo, W. A., Gruber, A., De Jeu, R. A. M., Wagner, W., Stacke, T., Loew, A., Albergel, C., Brocca, L., Chung, D., Parinussa, R. M., and Kidd, R.: Evaluation of the ESA CCI soil moisture product using ground-based observations, Remote Sensing of Environment, 162, 380-395, 2015.

Gruber, A., Dorigo, W. A., Zwieback, S., Xaver, A., and Wagner, W.: Characterizing Coarse-Scale Representativeness of in situ Soil Moisture Measurements from the International Soil Moisture Network, Vadose Zone Journal, 12, 0, 2013.

Haddeland, I., Skaugen, T., and Lettenmaier, D. P.: Hydrologic effects of land and water management in North America and Asia: 1700–1992, Hydrology and Earth System Sciences Discussions, 3, 2899-2922, 2007.

Hanes, J. M. and Schwartz, M. D.: Modeling land surface phenology in a mixed temperate forest using MODIS measurements of leaf area index and land surface temperature, Theoretical and Applied Climatology, 105, 37-50, 2010.

Huang, Y., Sheng Chen, Qing Cao, Yang Hong, Biwen Wu, Mengyu Huang, Lei Qiao, Zengxin Zhang, Zhe Li, and Yang, W. L. a. X.: Evaluation of Version-7 TRMM Multi-Satellite Precipitation Analysis Product during the Beijing Extreme Heavy Rainfall Event of 21 July 2012, Water, 6, 13, 2014.

Jiao, Y., Lei, H., Yang, D., Huang, M., Liu, D., and Yuan, X.: Impact of vegetation dynamics on hydrological processes in a semi-arid basin by using a land surface-hydrology coupled model, Journal of Hydrology, 551, 116-131, 2017.

Kirchner, J. W.: Getting the right answers for the right reasons: Linking measurements, analyses, and models to advance the science of hydrology, Water Resources Research, 42, 2006.

Kottek, M., Grieser, J., Beck, C., Rudolf, B., and Rubel, F.: World Map of the Köppen-Geiger climate classification updated, Meteorologische Zeitschrift, 15, 259-263, 2006.

Lee, K., Gao, H., Huang, M., Sheffield, J., and Shi, X.: Development and Application of Improved Long-Term Datasets of Surface Hydrology for Texas, Advances in Meteorology, 2017, 1-13, 2017.

Li, H., Wigmosta, M. S., Wu, H., Huang, M., Ke, Y., Coleman, A. M., and Leung, L. R.: A Physically Based Runoff Routing Model for Land Surface and Earth System Models, Journal of Hydrometeorology, 14, 808-828, 2013.

Liang, S., Zhao, X., Liu, S., Yuan, W., Cheng, X., Xiao, Z., Zhang, X., Liu, Q., Cheng, J., Tang, H., Qu, Y., Bo, Y., Qu, Y., Ren, H., Yu, K., and Townshend, J.: A long-term Global LAnd Surface Satellite (GLASS) data-set for environmental studies, International Journal of Digital Earth, 6, 5-33, 2013.

Liang, X., D. P. Lettenmaier, E. F. Wood, and S. J. Burges A simple hydrologically based model of land surface water and energy fluxes for general circulation models, J. Geophys. Res, 99(D7), 14, 1994.

Liang, X., E. F. Wood, and D. P. Lettenmaier Surface soil moisture parameterization of the VIC-2L model: Evaluation and modification, Global and Planetary Change, doi: 10.1016/0921-8181(95)00046-1, 1996. 1996.

Liang, X. and Xie, Z.: A new surface runoff parameterization with subgrib-scale soil heterogeneity for land surface models, Advances in Water Resources, 24, 1173-1193, 2001.

Liu, J., Liu, M., Zhuang, D., Zhang, Z., and Deng, X.: Study on spatial pattern of land-use change in China during 1995—2000, Science in China Ser D, 46, 373-384, 2003.

Liu, J., Zhang, Z., Xu, X., Kuang, W., Zhou, W., Zhang, S., Li, R., Yan, C., Yu, D., Wu, S., and Jiang, N.: Spatial patterns and driving forces of land use change in China during the early 21st century, Journal of Geographical Sciences, 20, 483-494, 2010.

Luo, X., Liang, X., and McCarthy, H. R.: VIC+ for water-limited conditions: A study of biological and hydrological processes and their interactions in soil-plant-atmosphere continuum, Water Resources Research, 49, 7711-7732, 2013.

Melsen, L. A., Teuling, A. J., Torfs, P. J. J. F., Uijlenhoet, R., Mizukami, N., and Clark, M. P.: HESS Opinions: The need for process-based evaluation of large-domain hyper-resolution models, Hydrology and Earth

Hydrol. Earth Syst. Sci. Discuss., https://doi.org/10.5194/hess-2019-72
Manuscript under review for journal Hydrol. Earth Syst. Sci.
Discussion started: 13 February 2019

Hydrology and Earth System Sciences
Open Access
Discussions

System Sciences, 20, 1069-1079, 2016.

Meng, S., Xie, X., and Liang, S.: Assimilation of soil moisture and streamflow observations to improve flood forecasting with considering runoff routing lags, Journal of Hydrology, 550, 568-579, 2017.

Mitchell, K. E.: The multi-institution North American Land Data Assimilation System (NLDAS): Utilizing multiple GCIP products and partners in a continental distributed hydrological modeling system, Journal of Geophysical Research, 109, 2004.

Mo, X., Wu, J. J., Wang, Q., and Zhou, H.: Variations in water storage in China over recent decades from GRACE observations and GLDAS, Natural Hazards and Earth System Sciences, 16, 469-482, 2016.

Nijssen, B., Lettenmaier, D. P., Lohmann, D., and Wood, E. F.: Predicting the Discharge of Global Rivers, Journal of Climate, 14, 3307-3323, 2000.

Nijssen, B., Schnur, R., and Lettenmaier, D. P.: Global Retrospective Estimation of Soil Moisture Using the Variable Infiltration Capacity Land Surface Model, 1980-93, Journal of Climate, 14, 1790-1808, 1999.

Pan, M., Sahoo, A. K., Troy, T. J., Vinukollu, R. K., Sheffield, J., and Wood, E. F.: Multisource Estimation of Long-Term Terrestrial Water Budget for Major Global River Basins, Journal of Climate, 25, 3191-3206, 2012.

Piao, S., Ciais, P., Huang, Y., Shen, Z., Peng, S., Li, J., Zhou, L., Liu, H., Ma, Y., Ding, Y., Friedlingstein, P., Liu, C., Tan, K., Yu, Y., Zhang, T., and Fang, J.: The impacts of climate change on water resources and agriculture in China, Nature, 467, 43-51, 2010.

Qin, Y., Yang, D., Lei, H., Xu, K., and Xu, X.: Comparative analysis of drought based on precipitation and soil moisture indices in Haihe basin of North China during the period of 1960–2010, Journal of Hydrology, 526, 55-67, 2015.

Qiu, J., Gao, Q., Wang, S., and Su, Z.: Comparison of temporal trends from multiple soil moisture data sets and precipitation: The implication of irrigation on regional soil moisture trend, International Journal of Applied Earth Observation and Geoinformation, 48, 17-27, 2016.

Rodell, M., P.R. Houser, U. Jambor, J. Gottschalck, K. Mitchell, C.-J. Meng, K. Arsenault, B. Cosgrove, J. Radakovich, M. Bosilovich, J.K. Entin, J.P. Walker, D. Lohmann, and Toll, D.: The Global Land Data Assimilation System, Bull. Amer. Meteor. Soc., 85, 381-394, 2004.

Scherer, L., Venkatesh, A., Karuppiah, R., and Pfister, S.: Large-scale hydrological modeling for calculating water stress indices: implications of improved spatiotemporal resolution, surface-groundwater differentiation, and uncertainty characterization, Environmental science & technology, 49, 4971-4979, 2015.

Shangguan, W., Dai, Y., Liu, B., Zhu, A., Duan, Q., Wu, L., Ji, D., Ye, A., Yuan, H., Zhang, Q., Chen, D., Chen, M., Chu, J., Dou, Y., Guo, J., Li, H., Li, J., Liang, L., Liang, X., Liu, H., Liu, S., Miao, C., and Zhang, Y.: A China data set of soil properties for land surface modeling, Journal of Advances in Modeling Earth Systems, 5, 212-224, 2013.

Shi, C. X., Xie, Z. H., Hui, Q., Liang, M. L., and Yang, X. C.: China land soil moisture EnKF data assimilation based on satellite remote sensing data, Science China Earth Sciences, 54, 1430-1440, 2011.

Strahler, A., Gopal, S., Lambin, E., and Moody, A.: MODIS Land Cover Product Algorithm Theoretical Basis Document (ATBD) MODIS Land Cover and Land-Cover Change, 1999. 1999.

Tesemma, Z. K., Wei, Y., Peel, M. C., and Western, A. W.: The effect of year-to-year variability of leaf area index on Variable Infiltration Capacity model performance and simulation of runoff, Advances in Water Resources, 83, 310-322, 2015.

Troy, T. J., Wood, E. F., and Sheffield, J.: An efficient calibration method for continental-scale land surface modeling, Water Resources Research, 44, 2008.

Umair, M., Kim, D., Ray, R. L., and Choi, M.: Estimating land surface variables and sensitivity analysis for CLM and VIC simulations using remote sensing products, Science of The Total Environment, 633, 470-483, 2018.

Wang, A., Lettenmaier, D. P., and Sheffield, J.: Soil Moisture Drought in China, 1950–2006, Journal of Climate, 24, 3257-3271, 2011.

Wang, G. Q., Zhang, J. Y., Jin, J. L., Pagano, T. C., Calow, R., Bao, Z. X., Liu, C. S., Liu, Y. L., and Yan, X. L.: Assessing water resources in China using PRECIS projections and a VIC model, Hydrology and Earth System Sciences, 16, 231-240, 2012.

Wang, K., Wang, L., Wei, Y.-M., and Ye, M.: Beijing storm of July 21, 2012: observations and reflections, Natural Hazards, 67, 969-974, 2013.

Wang, S., Mo, X., Liu, S., Lin, Z., and Hu, S.: Validation and trend analysis of ECV soil moisture data on cropland in North China Plain during 1981–2010, International Journal of Applied Earth Observation and Geoinformation, 48, 110-121, 2016.

Wen, Z., Liang, X., and Yang, S.: A new multiscale routing framework and its evaluation for land surface modeling applications, Water Resources Research, 48, 2012.

Wood, E. F., Roundy, J. K., Troy, T. J., van Beek, L. P. H., Bierkens, M. F. P., Blyth, E., de Roo, A., Döll, P., Ek, M., Famiglietti, J., Gochis, D., van de Giesen, N., Houser, P., Jaffé, P. R., Kollet, S., Lehner, B., Lettenmaier, D. P., Peters-Lidard, C., Sivapalan, M., Sheffield, J., Wade, A., and Whitehead, P.: Hyperresolution global land surface modeling: Meeting a grand challenge for monitoring Earth's terrestrial water, Water Resources Research, 47, 2011.

Wu, H., Adler, R. F., Tian, Y., Huffman, G. J., Li, H., and Wang, J.: Real-time global flood estimation using satellite-based precipitation and a coupled land surface and routing model, Water Resources Research, 50, 2693-2717, 2014.

Wu, J., Zhou, L., Mo, X., Zhou, H., Zhang, J., and Jia, R.: Drought monitoring and analysis in China based on the Integrated Surface Drought Index (ISDI), International Journal of Applied Earth Observation and Geoinformation, 41, 23-33, 2015.

Xie, X. and Cui, Y.: Development and test of SWAT for modeling hydrological processes in irrigation districts with paddy rice, Journal of Hydrology, 396, 61-71, 2011.

Xie, X., Liang, S., Yao, Y., Jia, K., Meng, S., and Li, J.: Detection and attribution of changes in hydrological cycle over the Three-North region of China: Climate change versus afforestation effect, Agricultural and Forest Meteorology, 203, 74-87, 2015.

Xie, Z., Yuan, F., Duan, Q., Zheng, J., Liang, M., and Chen, F.: Regional Parameter Estimation of the VIC Land Surface Model: Methodology and Application to River Basins in China, Journal of Hydrometeorology, 8, 447-468, 2007.

Xu, K., Yang, D., Yang, H., Li, Z., Qin, Y., and Shen, Y.: Spatio-temporal variation of drought in China during 1961–2012: A climatic perspective, Journal of Hydrology, 526, 253-264, 2015.

Yao, Y., Liang, S., Li, X., Chen, J., Wang, K., Jia, K., Cheng, J., Jiang, B., Fisher, J. B., Mu, Q., Grünwald, T., Bernhofer, C., and Roupsard, O.: A satellite-based hybrid algorithm to determine the Priestley–Taylor parameter for global terrestrial latent heat flux estimation across multiple biomes, Remote Sensing of Environment, 165, 216-233, 2015.

Yao, Y., Liang, S., Li, X., Yang, H., Fisher, J. B., Zhang, N., Chen, J., Jie, C., Zhao, S., and Zhang, X.: Bayesian multi-model estimation of global terrestrial latent heat flux from eddy covariance, meteorological and satellite observations, Journal of Geophysical Research Atmospheres, 119, 4521-4545, 2014.

Ye, T., Shi, P., Wang, J. a., Liu, L., Fan, Y., and Hu, J.: China's drought disaster risk management: Perspective

Hydrol. Earth Syst. Sci. Discuss., https://doi.org/10.5194/hess-2019-72
Manuscript under review for journal Hydrol. Earth Syst. Sci.
Discussion started: 13 February 2019

Hydrology and Earth System Sciences Discussions
Open Access

of severe droughts in 2009–2010, International Journal of Disaster Risk Science, 3, 84-97, 2012.

Yin, J., Zhan, X., Zheng, Y., Hain, C. R., Ek, M., Wen, J., Fang, L., and Liu, J.: Improving Noah land surface model performance using near real time surface albedo and green vegetation fraction, Agricultural and Forest Meteorology, 218-219, 171-183, 2016.

Zeng, Y., Xie, Z., Liu, S., Xie, J., Jia, B., Qin, P., and Gao, J.: Global Land Surface Modeling Including Lateral Groundwater Flow, Journal of Advances in Modeling Earth Systems, 10, 1882-1900, 2018.

Zeng, Y., Xie, Z., Yu, Y., Liu, S., Wang, L., Zou, J., Qin, P., and Jia, B.: Effects of anthropogenic water regulation and groundwater lateral flow on land processes, Journal of Advances in Modeling Earth Systems, 8, 1106-1131, 2016.

Zhai, P., Zhang, X., Wan, H., and Pan, X.: Trends in total precipitation and frequency of daily precipitation extremes over China, Journal of Climate, 18, 1096-1108, 2005.

Zhang, Q., Gu, X., Singh, V. P., Kong, D., and Chen, X.: Spatiotemporal behavior of floods and droughts and their impacts on agriculture in China, Global and Planetary Change, 131, 63-72, 2015.

Zhang, Q., Gu, X., Singh, V. P., Liu, L., and Kong, D.: Flood-induced agricultural loss across China and impacts from climate indices, Global and Planetary Change, 139, 31-43, 2016.

Zhang, X., Q. Tang, M. Pan, and Tang, Y.: A Long-Term Land Surface Hydrologic Fluxes and States Dataset for China, Journal of Hydrometeorology, doi: 10.1175/JHM-D-13-0170.1, 2014. 2014.

Zhang, Y., Xu, Y., Dong, W., Cao, L., and Sparrow, M.: A future climate scenario of regional changes in extreme climate events over China using the PRECIS climate model, Geophysical Research Letters, 33, 2006.

Zhang, Y., You, Q., Chen, C., and Li, X.: Flash droughts in a typical humid and subtropical basin: A case study in the Gan River Basin, China, Journal of Hydrology, 551, 162-176, 2017.

Zhao, X., Liang, S., Liu, S., Yuan, W., Xiao, Z., Liu, Q., Cheng, J., Zhang, X., Tang, H., Zhang, X., Liu, Q., Zhou, G., Xu, S., and Yu, K.: The Global Land Surface Satellite (GLASS) Remote Sensing Data Processing System and Products, Remote Sensing, 5, 2436-2450, 2013.

Zhu, B., Xie, X., and Zhang, K.: Water storage and vegetation changes in response to the 2009/10 drought over North China, Hydrology Research, doi: 10.2166/nh.2018.087, 2018. nh2018087, 2018.

Zhu, C. and Lettenmaier, D. P.: Long-Term Climate and Derived Surface Hydrology and Energy Flux Data for Mexico: 1925–2004, Journal of Climate, 20, 1936-1946, 2007.